Technical performance of lignin-modified bitumen and organic bitumen as binders for asphalt considering environmental criteria

Erik Kamratowsky [a], Chaoliang Fu [b, *], Sabine Leischner [a], Pamela Haverkamp [c], Marzia Traverso [c], Pengfei Liu [b]

[a] *Institute of Urban Planning and Pavement Engineering, Department of Civil Engineering, TU Dresden, 01062 Dresden, Germany*

[b] *Institute of Highway Engineering, RWTH Aachen University, 52074 Aachen, Germany*

[c] *Institute of Sustainability in Civil Engineering (INaB), RWTH Aachen University, 52074 Aachen, Germany*

* Corresponding Author: fu@isac.rwth-aachen.de

Abstract: Biomass-derived kraft lignin and organic bitumen have emerged as promising low-carbon alternatives to conventional petroleum-based bitumen, particularly in innovative "BioPave" applications. This study investigates the rheological behavior and environmental impact of lignin-modified bitumen and organic bitumen (natural asphalt blended with bio-oil) through a comparative analysis with conventional base bitumen. To achieve this, the chemical compositions of all bitumen samples, in both unaged and aged conditions, was first characterized using Fourier Transform Infrared (FTIR) spectroscopy to assess molecular structural changes due to oxidation. Subsequently, rheological properties were evaluated using dynamic shear rheometer (DSR) testing, focusing on the effects of aging on viscoelastic behavior. Furthermore, the environmental performances of the conventional and lignin-modified bitumen alternatives were assessed through Life Cycle Assessment (LCA) and compared with producer-specific environmental data for the organic bitumen. The results show that both bio-bitumen variants exhibit higher stiffness and improved rutting resistance, meeting heavy traffic requirements up to 70°C, with lignin-modified bitumen demonstrating superior aging resistance. LCA results indicate that organic bitumen reduces climate change impacts by nearly 50%, while lignin-modified bitumen achieves a 9.4% reduction. However, increased impacts in land use and resource consumption highlight the need for optimized biomass sourcing strategies. Overall, bio-bitumen presents a viable lower-carbon alternative with enhanced mechanical performance, though further research is required to optimize long-term durability and economic feasibility for practical implementation in road construction.

Keywords: Bio-bitumen; Natural asphalt; Rheological properties; Aging performance; Life cycle assessment

1. Introduction

The bioeconomy has rapidly emerged as a key sector and is now recognized in approximately 60 countries worldwide as a strategic pathway for mitigating climate change and addressing the depletion of

fossil fuel reserves (Global Bioeconomy Summit 2020, 2020). This approach is centered on replacing fossil-based products with bio-based alternatives while optimizing the use of global resources. As a by-product of petroleum refining, bitumen faces an urgent need for sustainable bio-based substitutes to lessen the dependence of pavement construction on limited petroleum resources, especially given the increasing demand for bitumen in road infrastructure and environmental concerns (Pahlavan et al., 2024).

Over the past few decades, bio-bitumen derived from bio-mass has emerged as a promising solution (Wang et al., 2020. Zhang et al., 2020). The total global lignin reserves are estimated to exceed 300 billion tons, with an annual growth of approximately 20 billion tons (Bruijnincx P., 2016). Lignin is the second most abundant natural polymer after cellulose. It is commonly found as a co-product of waste wood processing and a byproduct of the pulp and paper industries. The potential of lignin as a bitumen substitute was first explored by Terrel as early as 1980 (Terrel R., 1980). Since 2000, interest in incorporating lignin into asphalt has surged, with research focusing on its role as a modifier, filler, or partial bitumen replacement (Gaudenzi et al., 2023). Lignin can be introduced into asphalt via either the dry or wet method. In the dry process, lignin is added directly as a filler or modifier into the asphalt, requiring minimal adjustments to standard production methods. Pascoal et al. (2023) investigated the use of lignin waste, a by-product of bioethanol production from forest biomass, in warm-mix asphalt (WMA). Adding 20% lignin (by bitumen mass) via the dry process reduced the mixing temperature by 40°C without additional additives. In contrast, the wet process involves pre-mixing lignin with bitumen before mixture production, enhancing the binder's adhesive properties. Batista et al. (2018) explored commercial Kraft lignin-modified bitumen from the pulp and paper industry for pavement applications. Results showed that lignin increases viscosity, enhances rutting resistance, and improves thermal cracking resistance (up to -12°C). Modified binders demonstrated better aging, photodegradation, and thermal stability than conventional binders. Nahar et al. (2023) investigated the partial replacement of bitumen with native and chemically modified lignin (25 wt.%) derived from Kraft (Lignoboost softwood) and Organosolv (ethanol/water hardwood) processes. Their findings indicate that lignin generally increases binder stiffness, while ethyl hexyl glycidyl ether-modified lignin maintains viscoelastic properties comparable to the original bitumen. Furthermore, Tokede et al. (2020) compared the environmental performance cradle-to-gate of conventional asphalt and asphalt containing lignin binder. The results showed a 5.72% reduction in climate change due to the substitution of 25% of the bitumen binder with lignin.

Meanwhile, natural asphalt is emerged as a promising candidate for developing fully non-crude oil-based bitumen formulations (Rondón-Quintana et al., 2023). Among natural asphalts, gilsonite and Trinidad Lake Asphalt (TLA) are the most commonly utilized in pavement engineering. Sabouri et al. (2018) investigated the modification of PG 58-22 and PG 64-22 binders with varying gilsonite contents (4, 8, and 12 wt.%). Their findings indicated that gilsonite-enhanced asphalt exhibited improved fatigue life and

enhanced performance under medium and high-temperature conditions. Similarly, Ameli et al. (2021) analyzed the rheological and mechanical properties of gilsonite-modified bitumen and mixtures. Their study demonstrated that gilsonite incorporation significantly increased rutting resistance; however, it also led to reduced resistance to low-temperature cracking. Furthermore, rheological assessments revealed that higher gilsonite concentrations resulted in increased binder stiffness, viscosity, and resilience. In parallel, Sun et al. (2022) examined the effects of TLA on mastic asphalt and observed that TLA-modified binders exhibited superior high-temperature stability and reduced temperature susceptibility. Additionally, asphalt incorporating TLA demonstrated improved resistance to low-temperature cracking, highlighting the potential of TLA as an effective bitumen modifier. In addition, bio-oil is also considered a promising bio-bitumen for pavement construction due to its similar elemental composition to petroleum bitumen, as well as its inherent bonding properties and viscoelasticity. Several studies have evaluated the effects of vegetable oils on conventional binder properties, including penetration, softening temperature, rheological behavior (complex modulus, ductility, and creep performance), and fatigue resistance (Xu et al., 2023, Elahi et al., 2024). Sun et al. (2016) further investigated the chemical composition of vegetable oils and found that their asphaltene content is negligible (<1%), while their aromatic, resin, and saturated fractions closely resemble those of petroleum bitumen. Compatibility studies under static heating and storage conditions confirmed good miscibility between vegetable oils and bitumen, along with a notable improvement in stress relaxation. Additionally, Somé et al. (2016) developed novel bio-bitumen formulations by blending 71.4% natural bitumen, 17.9% vegetable waste oils, and 10.7% hard petroleum bitumen. Their study revealed that the bio-bitumen produced was softer than conventional P35/50 petroleum bitumen. The differential scanning calorimetry results showed that the addition of vegetable oils lowered the glass transition temperature of the final binders, thereby improving their low-temperature performance and resistance to thermal cracking.

In summary, despite recent advancements toward developing bitumen alternatives with lower environmental impacts, research on 100% non-crude oil-based bitumen remains limited. Most studies focus on partially replacing or modifying petroleum-based bitumen with bio-based components such as lignin, vegetable oils, or natural asphalt, rather than developing a fully bio-based binder. Furthermore, comparative studies evaluating the performance of 100% non-crude oil-based bitumen alongside conventional bitumen and lignin-modified bitumen are scarce. Additionally, comprehensive life cycle assessment (LCA) studies are necessary to evaluate the environmental sustainability of bio-bitumen throughout its production, application, and end-of-life stages. To address these gaps, this study systematically evaluates the potential of bio-bitumen as a more environmental alternative to fossil crude oil-based bitumen by comparing their chemical, rheological, mechanical, and environmental properties. Specifically, two types of bio-bitumen are investigated: a 20% bio-bitumen (bitumen 50/70 with wt.% Kraft lignin) and an organic bitumen (comprising natural asphalt and vegetable oil). The research methodology includes chemical composition

and aging analysis using Fourier Transform Infrared Spectroscopy (FTIR), viscoelastic behavior assessment through dynamic shear rheometer tests using the 2S2P1D model, and plastic deformation resistance evaluation via creep testing at elevated temperatures. Furthermore, a cradle-to-gate LCA is conducted for the conventional and lignin-modified bitumen alternatives. The outcomes are then compared to producer-specific environmental data of the organic bitumen to identify potential improvements in the environmental performance.

2. Materials and sample preparation

2.1 Lignin-modified bitumen

To investigate the effect of lignin on the performance of base bitumen, samples were prepared by incorporating 20 wt.% Kraft lignin into the base bitumen. The base bitumen used in this study had a penetration grade of 50/70 and a softening point of 54.8°C. The Kraft lignin, with a density of 1.3 g/cm^3, was obtained as a byproduct of the pulp and paper industry and was supplied by the Pontifical Catholic University of Chile. Kraft lignin exhibits an irregular surface morphology, as revealed by scanning electron microscopy (SEM). The microscopic analysis shows that its particle structures resemble common asphalt fillers such as limestone or granodiorite, suggesting that Kraft lignin may function not only as a bitumen modifier but also as a filler material in asphalt. The primary chemical composition of Kraft lignin includes 0.20% nitrogen, 63.60% carbon, 5.70% hydrogen, and 1.40% sulfur, with a specific surface area (SSA) of 1.12 m^2/g.

The production of a homogeneous lignin-modified bitumen presents several challenges, primarily due to the hydrophilic nature of lignin, which affects its compatibility with bitumen. Therefore, strict control over mixing parameters, such as temperature and rotation speed, is essential to ensure proper dispersion and integration. Through preliminary research, the optimal preparation conditions were determined to be a constant mixing temperature of 135°C, a rotation speed of 5000 rpm, and a mixing duration of 60 minutes. Additionally, to reduce moisture content and enhance lignin dispersion, the lignin was pre-dried in an oven at 60°C for 60 minutes before mixing. These optimized conditions significantly improved the uniformity and stability of the lignin-bitumen blend, ensuring better performance in subsequent analyses.

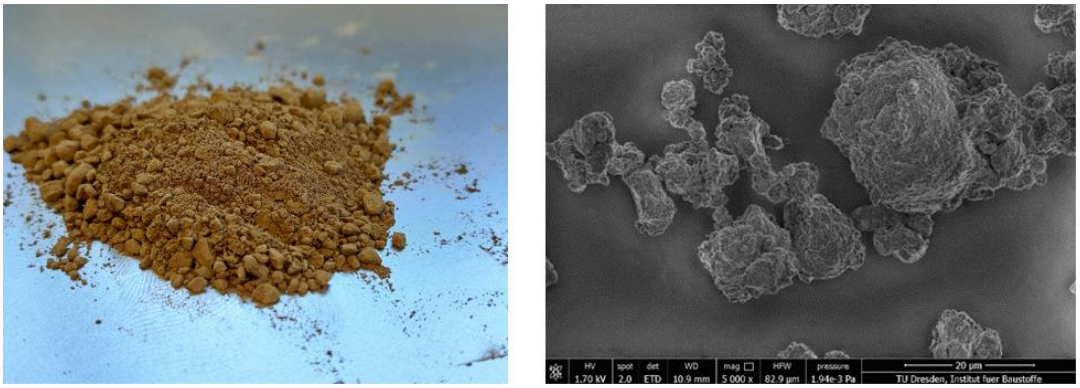

Fig. 1 Kraft lignin powder and SEM image of kraft lignin

2.2 Organic bitumen

The 100% non-crude oil-based bitumen, referred to as organic bitumen in this study, is composed of natural asphalt (Fig. 2) and plant-based bio-oil. The bio-oil is cashew nut shell liquid (CNSL), which is derived from unsaturated phenols and is a byproduct of the cashew nut industry. Previous studies have shown that CNSL enhances bitumen performance by reducing stiffness, improving compatibility with additives, and enhancing rutting resistance in asphalt (Ribeiro et al., 2012).

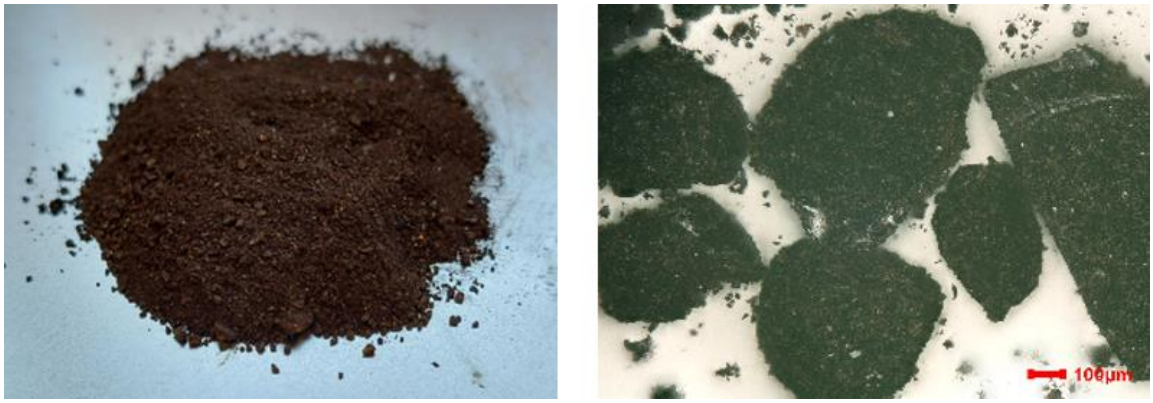

Fig. 2 Natural asphalt and video microscope image of natural asphalt

The hardness of organic bitumen can be adjusted by modifying the natural asphalt-to-CNSL ratio. A 45:55 ratio (natural asphalt-to-CNSL, by weight) produces a 50/70 penetration-grade bitumen, while a 48:52 ratio results in a 70/100 penetration-grade bitumen. To facilitate a direct comparison with conventional 50/70 bitumen, this study employed the 45:55 ratio following the recommendations of the producer of the organic bitumen. It can be assumed that organic maintains mechanical properties similar to conventional petroleum-based bitumen, making it a viable alternative in pavement applications.

The production of organic bitumen in the laboratory followed a controlled mixing process to ensure homogeneity while minimizing volatile component loss. Initially, natural asphalt and CNSL were manually mixed at room temperature. A high-speed shear mixer was then used to achieve uniform dispersion. The mixing process parameters were carefully optimized: the mixture was stirred at 3000 rpm for 12 minutes, with the temperature raised to 145°C. After this, the sample was cooled to 120°C using a reduced mixing speed of 1000 rpm for 15 minutes to prepare it for subsequent testing. This optimized preparation method ensured the production of a stable and homogeneous organic bitumen, suitable for performance evaluation and practical application in asphalt.

2.3 Aging simulation of bio-bitumen

To assess the aging performance of bio-bitumen, including lignin-modified bitumen, organic bitumen, and 50/70 base bitumen, the Rolling Thin Film Oven (RTFO) test was used to simulate the short-term aging that occurs during the mixing and construction phases. In accordance with EN 12607-1 (European Committee for Standardization, 2014), the bio-bitumen samples were subjected at 163°C for 75 minutes.

For clarity, the bitumen samples before and after aging were systematically categorized and assigned specific designations, as presented in Table 1.

Table 1 Materials analyzed in this study

Sample ID	Description
50/70	Unaged 50/70 base bitumen
50/70 RTFO	Aged 50/70 base bitumen
50/70 L	Unaged 50/70 base bitumen with 20% Kraft lignin
50/70 L RTFO	Aged 50/70 base bitumen with 20% Kraft lignin
OB	Unaged 100% Organic bitumen
OB RTFO	Aged 100% Organic bitumen

3. Experimental methodology

3.1 Fourier-Transform Infrared Spectroscopy tests

In this study, Fourier Transform Infrared Spectroscopy (FTIR) was employed to investigate the oxidation-induced structural changes in bitumen samples, the interaction between lignin and bitumen components, and the synergistic effects of bio-oil and natural asphalt on the material's aging resistance and overall chemical stability. The infrared spectra were recorded using a Perkin Elmer Spectrum Two™ FTIR spectrometer, which is equipped with an attenuated total reflectance (ATR) unit and a diamond crystal. To ensure reliable measurements, each bitumen sample was briefly heated (1–2 minutes) to achieve homogeneity, mixed using a spatula, and prepared drop by drop for analysis. To minimize additional aging caused by UV exposure, the samples were immediately covered after preparation. Before measurement, the samples were allowed to cool for 10 minutes to ensure consistency in spectral acquisition. The spectra were recorded over a wavenumber range of 4000 cm^{-1} – 400 cm^{-1}, with a resolution of 4 cm^{-1}, and 32 scans per measurement were conducted to enhance signal accuracy. Each bitumen variant was tested using four individual samples, with a new background spectrum recorded before each measurement to eliminate external interferences. After acquisition, the spectra were normalized by setting the aliphatic peak (the most intense band at approximately 2920 cm^{-1}) to a value of 2, while the global minimum was set to 0, ensuring consistency in spectral interpretation.

To quantify the extent of chemical aging, the chemical aging state of the bitumen samples was quantified by analyzing the spectral intensities of two key oxidation-related functional groups, including carbonyl (C=O) group and sulfoxide (S=O) group. The carbonyl (C=O) group, which is associated with oxidative aging, exhibits an absorption band at 1700 cm^{-1}, while the sulfoxide (S=O) group, linked to oxidation and degradation, displays a stretching vibration at 1030 cm^{-1}. These functional groups are widely recognized as indicators of bitumen oxidation, reflecting aging progression over the material's lifetime. In this case, the Aging Index (AI_{FTIR}) was expressed by Eq. (1) (Mirwald et al. 2022).

$$AI_{FTIR} = \frac{AI_{CO} + AI_{SO}}{AI_{CH3}} \quad (1)$$

where AI_{CO} corresponds to the integration range of the carbonyl group, AI_{SO} represents the integration range of the sulfoxide group, and AI_{CH3} denotes the integration range of the aliphatic bands.

3.2 Rheological tests

3.2.1 Frequency-Temperature sweep tests

The temperature-frequency (TF) sweep tests were used to assess the rheological characteristics of lignin-modified bitumen and organic bitumen using frequencies ranging from 0.16 to 15.92 Hz and temperatures from -10 °C to 70 °C. The configuration geometry of the testing parallel plate was 8 mm in diameter with a 2 mm gap, and the testing temperature range was -10°C to 40°C. The 25 mm diameter with a 1 mm gap configuration was used for elevated temperatures ranging from 30°C to 70°C. The raw data was interpreted in the form of master curves that describe the temperature-frequency dependence of the dynamic shear modulus (|G*|) and the phase angle (δ). In accordance with the time-temperature superposition principle (TTSP), when a test temperature condition is difficult to achieve in practice, a suitable temperature can be taken as a reference temperature, and the frequency at other temperatures can be transformed into the reduced frequency at the reference temperature (Lin et al., 2022). Therefore, the dynamic shear modulus and phase angle at other temperatures can be equivalent to those of the reduced frequency at the reference temperature, respectively. The time-temperature equivalent factor equation used in this study was Williams-Landel-Ferry (WLF) equation

$$\log(a_T) = \frac{C_1 \cdot (T - T_{ref})}{C_2 + (T - T_{ref})} \quad (2)$$

$$\omega_r = a_T \times \omega \quad (3)$$

where a_T is the time-temperature equivalent factor; C_1 and C_2 are the fit parameters; T and T_{ref} are the actual test temperature and the reference temperature (20 °C), respectively; ω_r and ω are the actual test angular frequency and reduced angular frequency, respectively.

Based on the TTSP, the 2S2P1D model (Li et al., 2022) shows an outstanding correlation between the measured and fitted data for modified bitumen, and is used to evaluate the rheological behavior of lignin-modified bitumen and organic bitumen. The 2S2P1D model consists of seven parameters and the $|G^*|$ is shown in the following expression:

$$G^*(\omega) = G_o + \frac{G_g - G_o}{1 + \alpha(i\omega\tau)^{-k} + (i\omega\tau)^{-h} + (i\omega\beta\tau)^{-1}} \quad (4)$$

where k and h are dimensionless parameters with $0 < k < h < 1$; α is constant; G_o is the static modulus when $\omega \to 0$, G_g is the glassy modulus when $\omega \to \infty$; β is a parameter related to Newtonian viscosity.

In addition, two aging indices were introduced to evaluate the aging behavior of bituminous materials. The first index, termed the changing index (CI), is used to compare the aging sensitivity among different binders by using the base bitumen as a reference. The CI is defined as follows:

$$CI = \frac{B_{bio}}{B_b} \tag{5}$$

where B_{bio} represents the measured property (such as the complex shear modulus or phase angle) of the bio-bitumen (e.g., lignin-modified bitumen or organic bitumen) and B_b represents the corresponding property of the base bitumen. This index provides a means to determine the relative aging sensitivity of bio-bitumen compared to the conventional bitumen.

The second indicator is an aging index (AI) that compares the performance of each binder before and after aging. This index is defined as the ratio between a specific property (such as the complex shear modulus or phase angle) measured on the aged binder and the same property measured on the unaged binder, as shown below:

$$AI = \frac{P_{aged}}{P_{unaged}} \tag{6}$$

where P_{aged} is the complex shear modulus or phase angle of three types of measured under aged conditions and P_{unaged} is the same property measured prior to aging.

3.2.2 SSCR tests

To characterize the resistance to permanent deformation, single stress creep and recovery (SSCR) tests were conducted following AASHTO T 350 (American Association of State Highway and Transportation Officials, 2019). Test temperatures ranged from 40 °C to 80 °C, chosen to represent a broad spectrum of in-service conditions and to ensure that the material undergoes non-linear viscoelastic behavior (Singh et al., 2023). A stress of 3.2 kPa was applied for 1 s, followed by a 9 s recovery period, with 10 load cycles performed at each temperature. This testing approach assesses the binder's ability to resist plastic (permanent) deformation while accounting for viscoelastic recovery. Two key parameters were derived: the percentage recovery *R* and the non-recoverable creep compliance J_{nr}. These were calculated for each load cycle using Eqs. (7) and (8),

$$R = \frac{\varepsilon_1 - \varepsilon_{10}}{\varepsilon_1} * 100 \tag{7}$$

$$J_{nr} = \frac{\varepsilon_{10}}{100 * 3.2} \tag{8}$$

where ε_1 is the strain at the end of the loading phase (1 s), and ε_{10} is the strain at the end of the unloading phase (10 s). Mean values of R and J_{nr} were then obtained by averaging over all 10 cycles at each temperature.

4. Life cycle assessment

To assess the environmental impacts and potential improvements of the bio-bitumen used in this study, a life cycle assessment (LCA) was implemented to quantify the environmental impacts of the product from cradle to gate, considering all relevant material and energy flows (Liljenström et al., 2022, Del Rosario P. & Traverso M., 2023, Zhang et al., 2025). An LCA study, in accordance with ISO 14040 (ISO, 2006a) and ISO 14044 (ISO, 2006b), consists of four key phases: goal and scope definition, life cycle inventory (LCI), life cycle impact assessment (LCIA), and interpretation. The goal and scope definition phase establishes the study's objectives and methodological framework, including the functional unit (i.e., the reference unit for assessment), system boundaries, key assumptions, and exclusions. Next, in the LCI phase, data collection is conducted in accordance with the defined reference unit and system boundaries. The LCIA phase follows, where classification and characterization of environmental impacts are carried out. Finally, in the interpretation phase, the results are analyzed in relation to the initial goal and scope, and sensitivity analysis and suggestions for improvements are provided. The subsequent sections detail the LCA procedure applied to the environmental assessment of the selected materials.

4.1 Goal and scope definition

The aim of this study was to quantify the environmental performance of selected material alternatives—bitumen 50/70, organic bitumen, and lignin-modified bitumen—by identifying environmental hotspots and evaluating potential trade-offs. The assessment followed the ISO 14040 and ISO 14044 standards (ISO, 2006a; ISO, 2006b). A functional unit of 1 ton of binder was chosen as the reference for the evaluation. A cradle-to-gate approach was adopted, encompassing the life cycle stages of raw material extraction, transportation, and the mixing process. The system boundaries of the assessment of the conventional and lignin-modified binders is shown in Fig.3. The system boundaries considered for the organic bitumen are also cradle-to-gate.

The assessment was conducted using GaBi© ts 10.6.2.9. A combination of primary and secondary data was used in the study. Primary data was used to model the mixing process of the modified bitumen, whereas secondary data, sourced from literature and the LCA databases Ecoinvent 3.8 and GaBi© Professionals v.2022.2, were used for the remaining materials and processes, unless otherwise stated. Bitumen 50/70 production was modelled based on the most recent LCI report from Eurobitume available at the time of the study (2020). The Eurobitume LCI was adapted to include crude oil transport, assumed to be imported from South America, covering 13,270 km covered by ship and 413 km by truck.

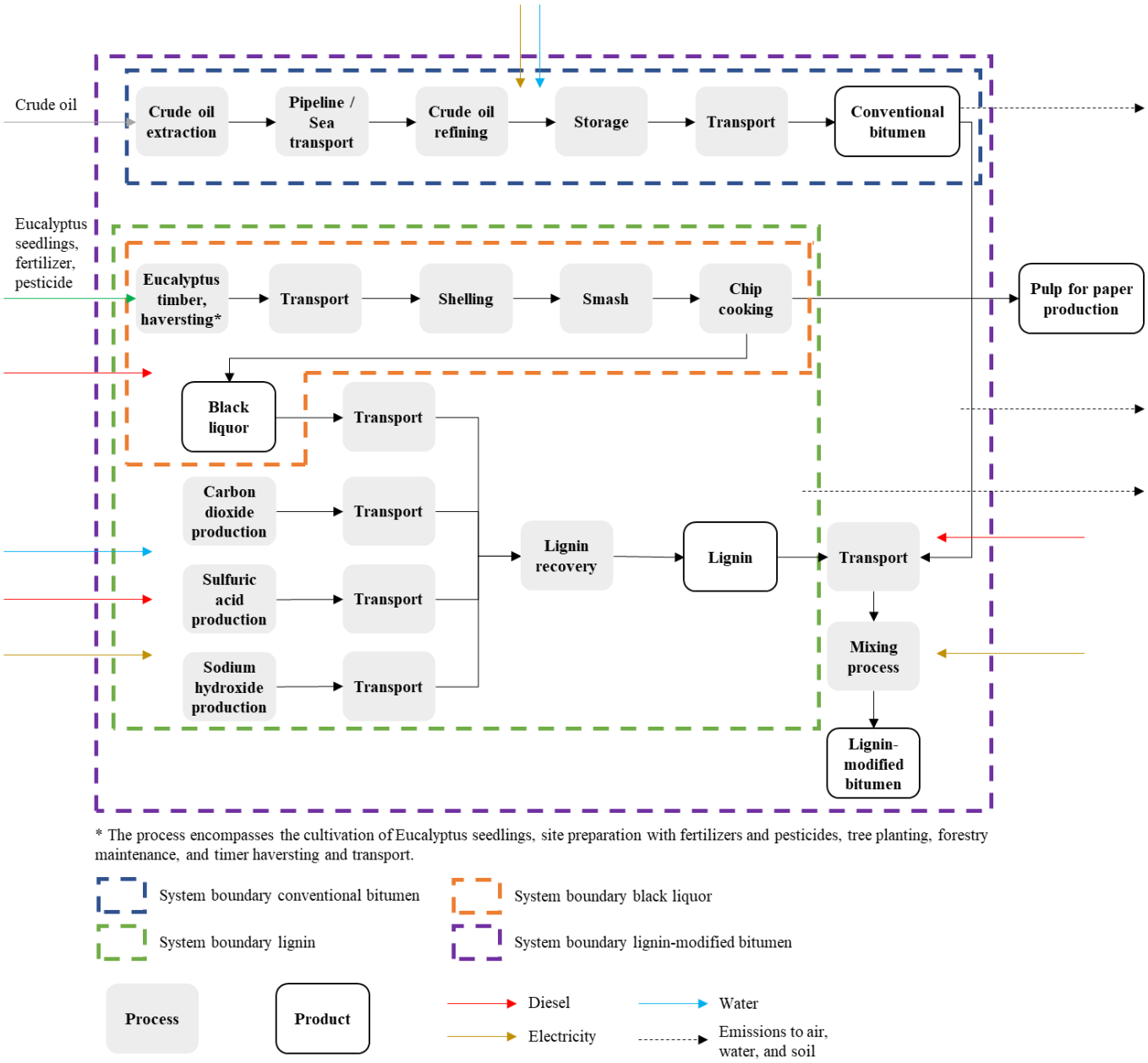

Fig. 3 System boundaries of conventional and lignin-modified bitumen based on Eurobitume (2020), Parvan (2023), and Liang et al. (2023)

In addition, the production of lignin requires black liquor, a by-product of kraft paper manufacturing. Black liquor is typically utilized by paper producers for energy generation (Fachagentur Nachwachsende Rohstoffe, 2025; Mantau et al., 2013). According to Liang et al. (2023), the production of 1 ton of kraft paper generates 11.2 tons of black liquor. Due to the significant mass discrepancy between the main product (paper) and the by-product (black liquor), a mass-based allocation approach was deemed inappropriate for distributing environmental burdens. Instead, an economic-based allocation method was considered. However, since black liquor is primarily used internally within the paper industry and does not typically enter the market, no reliable economic valuation was available. Some sources even indicate that black liquor has no commercial value (Fachagentur Nachwachsende Rohstoffe, 2025; Mantau et al., 2013). As a result,

it was assumed that black liquor has an economic value of zero. Consequently, all environmental impacts were attributed to the primary product (paper), while black liquor was considered burden-free within the lignin product system. To assess the impact of this allocation choice on the results, a sensitivity analysis was conducted during the interpretation phase (Section 4.4). Finally, the energy consumption required for mixing the lignin-modified bitumen was estimated at 0.56 kWh, based on the methodology outlined in the referenced study.

The Environmental Footprint (EF) 3.0 impact assessment method was employed to quantify the environmental impacts associated with bitumen 50/70 and lignin-modified bitumen. The characterized results are reported across all impact categories defined by EF 3.0 (Section 5.4.1). However, for organic bitumen, only the climate change impact category is reported, as it was the only available value for this material.

4.2 Life cycle inventory

The datasets used for modelling the material and energy inputs for the production and transport of bitumen 50/70 are presented in Table 2.

Table 2 Datasets used to model the production of bitumen 50/70

Input / Process	Dataset
Crude oil	DE: Crude oil mix Sphera
Natural gas	DE: Natural gas mix Sphera
Coal	DE: Hard coal mix Sphera
Water	EU-28: Process water from surface water Sphera
Ship transport	GLO: Container ship, 5,000 to 200,000 dwt payload capacity, ocean going
Ship fuel	EU-28: Process water from surface water Sphera
Truck transport	GLO: Truck, Euro 6, 28 - 32t gross weight / 22t payload capacity
Truck fuel	DE: Diesel mix at filling station Sphera

The kraft lignin used in the lignin-modified bitumen was modeled based on the methodology described in Parvan (2023). The corresponding datasets for this modeling are presented in Table 3.

Table 3 Datasets used for lignin production modeling

Input / Process	Dataset	Comment
Carbon dioxide	DE: Carbon dioxide by-product ethylene oxide (EO) via O2/methane Sphera	No country-specific dataset available. Several options were available, worst-case scenario was chosen.
Sulfuric acid	Sulfuric acid H2SO4 (96%) <e-ep>	
Sodium hydroxide	DE: Sodium hydroxide (from chlorine-alkali electrolysis, diaphragm) Sphera	No country-specific dataset available. Several options were available, worst-case scenario was chosen.

Input / Process	Dataset	Comment
Diesel	DE: Diesel mix at filling station Sphera	No country-specific dataset available.
Electricity	CL: Electricity grid mix Sphera	
Mill water	EU-28: Process water from surface water Sphera	No country-specific dataset available.
Tap water	DE: Tap water from surface water Sphera	No country-specific dataset available.

For the organic bitumen, no inventory data was available. However, a producer of this material provided a value for the impact category climate change that aligns with part of the system boundaries (raw material extraction and transport) defined in this study. The energy required to mix the components of the organic bitumen was estimated to be 0.15 kWh.

5. Results and discussions

5.1 Fourier-Transform Infrared Spectroscopy tests

Fig. 4 presents the FTIR spectra of the analyzed bitumen samples. The modification of base bitumen (50/70) with lignin induces notable changes in the FTIR spectrum. Compared with the base bitumen, the broad O–H stretching band (phenolic and aliphatic structures) between 3550 and 3100 cm^{-1} indicates an increased concentration of hydroxyl groups, which enhances the polarity of the system. Meanwhile, this modification is further evidenced by the enhanced aromatic C=C stretching at 1600 cm^{-1} and the emergence of a peak at 1512 cm^{-1}, both of which confirm the successful incorporation of lignin's polyaromatic framework. Additionally, characteristic peaks corresponding to the guaiacyl (1260 cm^{-1}) and Ar-CH in plane deformation (syringyl) at 1125 cm^{-1} further validate the presence of lignin. A substantial increase in the band at 1,030 cm^{-1} is observed following lignin modification. This band corresponds to the sulfoxide group (S=O), suggesting the presence of oxygen-containing compounds that undergo progressive aging in bitumen. The intensification of this band may be attributed to thermal stress during manufacturing. However, a review of the literature indicates that additional oxygen-containing compounds, especially those derived from kraft lignin, could also contribute to this increase. At this wavenumber, C–O(H) and C–O(C) deformations (first-order aliphatic OH or ether) are also apparent. Furthermore, a peak at 1,700 cm^{-1} is identified, representing the carbonyl group (C=O), which serves as another indicator of aging progression (Boeriu et al., 2004, Ibrahim et al., 2019).

Analysis of the organic bitumen reveals pronounced differences across the entire spectrum, especially in the fingerprint region, compared to the other two binders. The spectrum shows a distinct shift from the baseline, resulting in elevated absorption values in this region. The organic bitumen is produced by combining two components: Gilsonite natural asphalt (an asphaltene phase) and cashew shell nut oil (a maltene phase). A broad band at 3,350 cm^{-1} is indicative of C–H stretching, attributable to the maltene phase. C–H stretching is also evident around 3,075 cm^{-1}. Three bands at 3,100 cm^{-1}, 2,920 cm^{-1}, and 2,850

cm^{-1} result from asymmetric and symmetric C–H stretching. Alongside the aromatic peak at 1,600 cm^{-1}, additional bands at 1,590 cm^{-1} and 1,455 cm^{-1} correspond to aromatic stretching vibrations relative to bitumen 50/70. A peak at 1,485 cm^{-1} arises from CH_2 and CH_3 groups. A new peak at 1,265 cm^{-1} is attributed to phenolic C–O stretching. The band at 1,075 cm^{-1} is assigned to O–H bending vibrations, whereas the bands at 995 cm^{-1} and 910 cm^{-1} are associated with C–H stretching. A minor band at 750 cm^{-1} is also detected, corresponding to Ar–H stretching or aromatic rings (Achi et al., 2011, Srivastava R. & Srivastava D., 2015, Kyei et al., 2019,). Owing to the asphaltene phase, CH stretching vibrations at 2,920 cm^{-1} and 2,850 cm^{-1} are also visible. Two bands at 1,375 cm^{-1} and 1,450 cm^{-1} emerge due to bending frequencies and asymmetric C–CH_3 and/or methyl, as well as symmetric C–CH_3 bending vibrations (Ncir et al., 2014, Pakdaman et al., 2019). Neither the organic bitumen nor the base bitumen (50/70) shows a discernible peak at the carbonyl group (1,700 cm^{-1}). The sulfoxide group (1,030 cm^{-1}) exhibits a similar pattern to that of bitumen 50/70, yet displays higher absorption values due to the overall shift of the organic spectrum from the baseline.

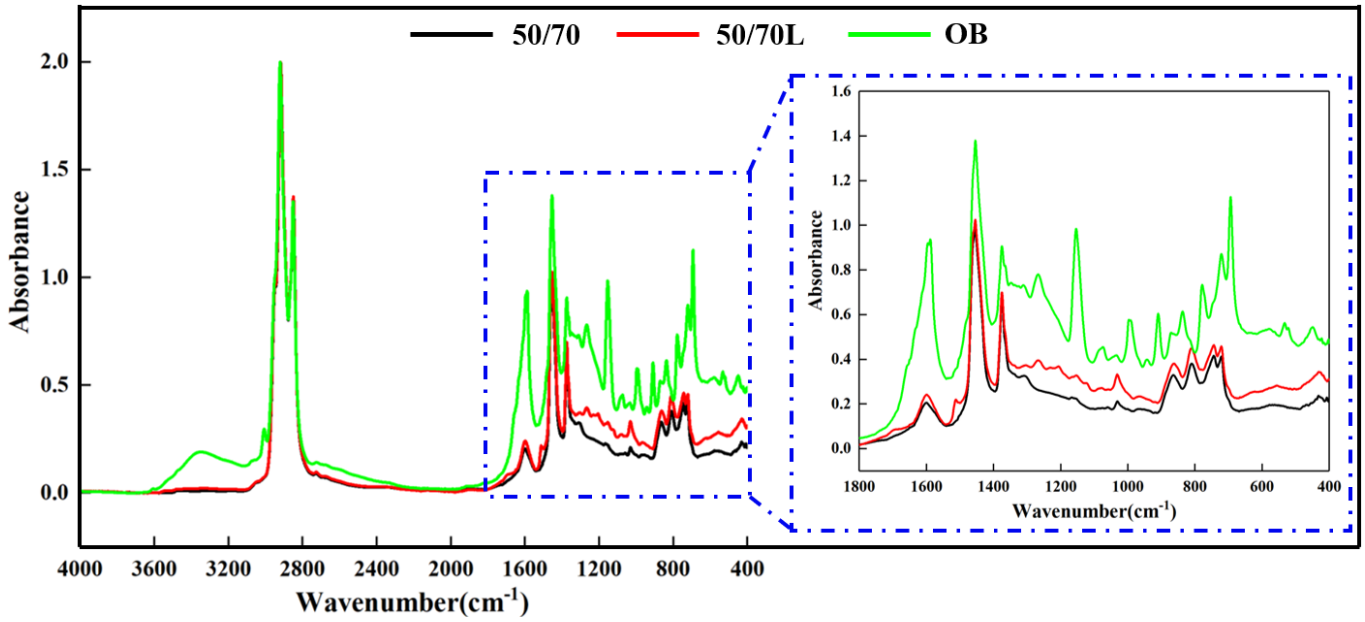

Fig. 4 Spectra of the unaged bitumen

Fig. 5 presents the FTIR spectra of the three binders—50/70 RTFO, 50/70L RTFO, and OB RTFO—after undergoing an RTFO aging procedure. All binders exhibit the typical signs of oxidative aging, most notably the increase in absorption around 1700 cm^{-1} (carbonyl groups, C=O) and at approximately 1030 cm^{-1} (sulfoxide groups, S=O). These bands are recognized indicators of the oxidative processes that bitumen undergoes under thermal, oxygen, and UV stress. Additionally, minor changes in the aromatic C–H stretching region (3050–3000 cm^{-1}) and in the fingerprint region (below 1500 cm^{-1}) provide further evidence of molecular rearrangements and the formation of new oxidation products. In the base bitumen, the intensity of the carbonyl band at 1700 cm^{-1} increases compared to the unaged sample, indicating a higher concentration of ketones, aldehydes, and carboxylic acids formed during aging. The sulfoxide band

near 1030 cm^{-1} also becomes more pronounced, reflecting sulfur-containing oxidation products. These observations align with the well-known oxidation mechanisms in bitumen, where the maltene fraction undergoes chemical changes that ultimately affect the asphaltene-maltene balance and may lead to increased stiffness and brittleness over time. The lignin-modified bitumen similarly shows intensified carbonyl and sulfoxide peaks upon aging, yet the relative magnitudes can differ from those in the base bitumen. Lignin contains phenolic structures, which can act as radical scavengers and potentially slow down the oxidative process. This antioxidant effect may manifest as a less pronounced rise in the carbonyl peak relative to the unmodified binder, depending on the amount and type of lignin used. However, lignin's aromatic rings and hydroxyl groups can themselves be susceptible to oxidation under severe conditions, sometimes leading to new or shifted peaks in the fingerprint region (e.g., around 1260 cm^{-1} for guaiacyl units). Consequently, the net aging behavior of 50/70L reflects a balance between lignin's potential protective role and the formation of additional oxidation products within its complex aromatic network. By contrast, the organic bitumen (OB)—a combination of gilsonite (asphaltene phase) and cashew shell nut oil (maltene phase)—displays a pronounced baseline shift and generally higher absorption values in the fingerprint region, just as it did in its unaged state. Upon aging, the carbonyl band around 1700 cm^{-1} and the sulfoxide band near 1030 cm^{-1} both increase in intensity, suggesting that oxidation affects both the high-aromatic gilsonite component and the unsaturated or phenolic fractions derived from cashew shell nut oil. The maltene phase may be particularly prone to oxidation, contributing to stronger carbonyl signals, while gilsonite's aromatic content can lead to additional sulfoxide formation. Overall, the interplay of these components governs OB's aging behavior, potentially preserving some favorable properties (e.g., flexibility or adhesion) but still exhibiting clear oxidative changes over time.

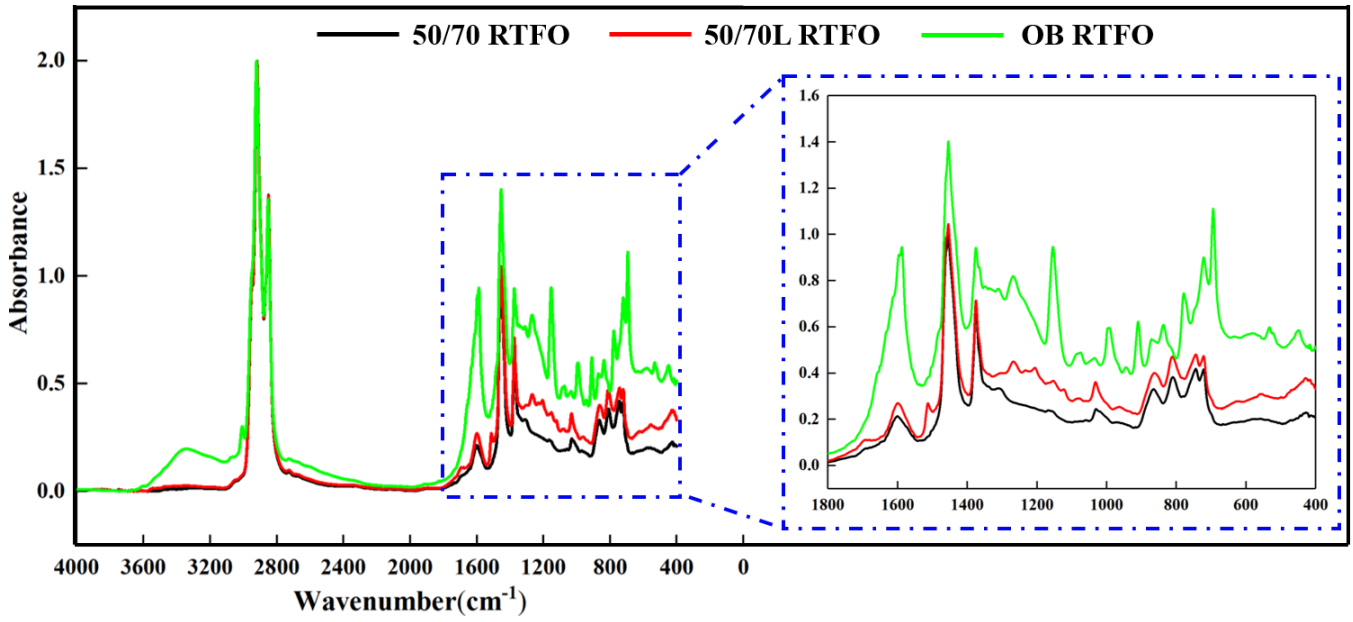

Fig. 5 Spectra of the aged bitumen

Fig. 6 presents the AI_{FTIR} values of three types of bitumen used in this study. Among the unaged samples, 50/70 exhibits the lowest AI_{FTIR}, suggesting that it contains fewer oxidation-related functional groups initially. By contrast, the higher AI_{FTIR} values observed in 50/70L and OB can be attributed to additional thermal stress during mixing and the inherent presence of oxygenated or aromatic structures in these binders. Notably, although 50/70L is the only binder showing a pronounced carbonyl peak, its overall aging index is still lower than that of OB. One explanation is that the bitumen-based integration limits used to calculate AI_{FTIR} may not fully capture the unique functional groups present in OB, thus affecting direct comparisons. To evaluate short-term aging resistance more effectively, the AI_{FTIR} change rate was introduced. This parameter represents the difference in AI_{FTIR} values between the short-term aged (RTFO) binder and the corresponding fresh (unaged) binder. As shown in red line in Fig. 6, 50/70L demonstrates the smallest increase in AI_{FTIR} after RTFO aging, indicating the greatest resistance to short-term aging, followed by OB. In contrast, 50/70 experiences the most significant rise in AI_{FTIR}, signifying its comparatively lower aging resistance.

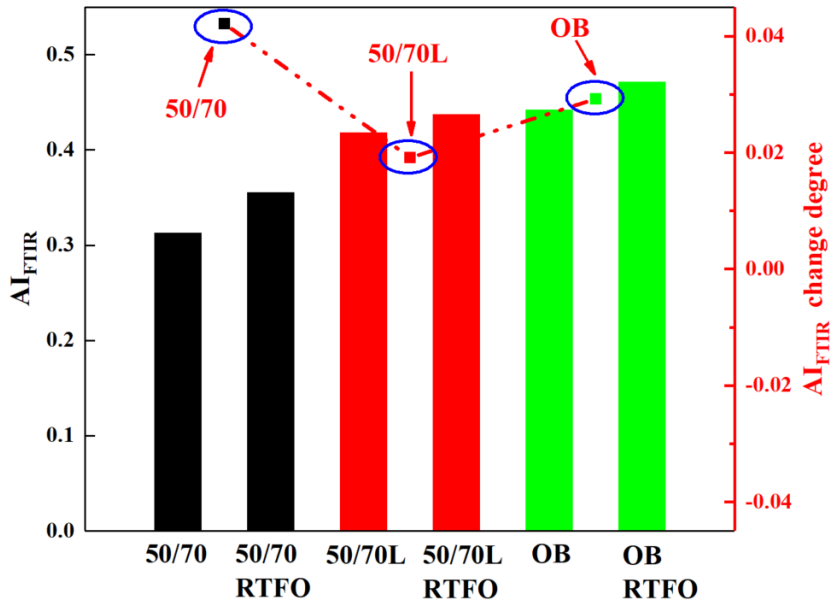

Fig. 6 Aging indices and their rate of change for three types of bitumen

5.2 Frequency-Temperature sweep tests

5.2.1 Black diagrams

Fig. 7 presents black diagrams comparing the rheological evolution of three binders before and after aging. These diagrams correlate the phase angle (δ) with the complex shear modulus (G*) on a logarithmic scale, integrating temperature- and frequency-dependent data into unified curves. In the unaged and aged state, all binders follow characteristic curves where higher G* (stiffness) corresponds to lower δ (more elastic behavior). Among them, the results show almost identical curves for the bitumen 50/70 and for the lignin-modified bitumen and a shift of the curve for the organic bitumen to lower values of the phase angle for shear moduli less than 100,000 MPa, i.e. at temperatures > 30°C. This is due to the double effect of the

increase in the complex shear modulus and the decrease in the phase angle at high temperatures. The first effect indicates an increase in the stiffness of the bitumen, the second an increase in the elastic behavior of the organic in this temperature range. This dual effect—higher G* and reduced δ—likely stems from bio-oil modification, which enhances high-temperature elasticity but may promote brittleness. Meanwhile, in certain portions of the data, the lignin-modified binder (50/70 L) exhibits a higher phase angle than the 50/70 binder at the same G*. This indicates that, under those specific frequency-temperature combinations, 50/70 L may behave more viscously (i.e., less elastically) than 50/70.

As shown in Fig. 7 (b), upon aging, all binders typically shift toward higher stiffness and lower phase angles, signifying a more elastic but also more brittle response. Oxidative aging processes increase the formation of polar, oxygenated species, leading to a stiffening effect. This shift is most apparent for the 50/70 binder because it lacks additional protective components, whereas 50/70 L's lignin component may mitigate oxidative effects via phenolic antioxidants. Moreover, organic bitumen's phase angle decreases significantly at a given G*, it suggests the binder has become more elastic and may be better at resisting permanent deformation (rutting), albeit potentially at the expense of flexibility at lower temperatures or under repeated loading.

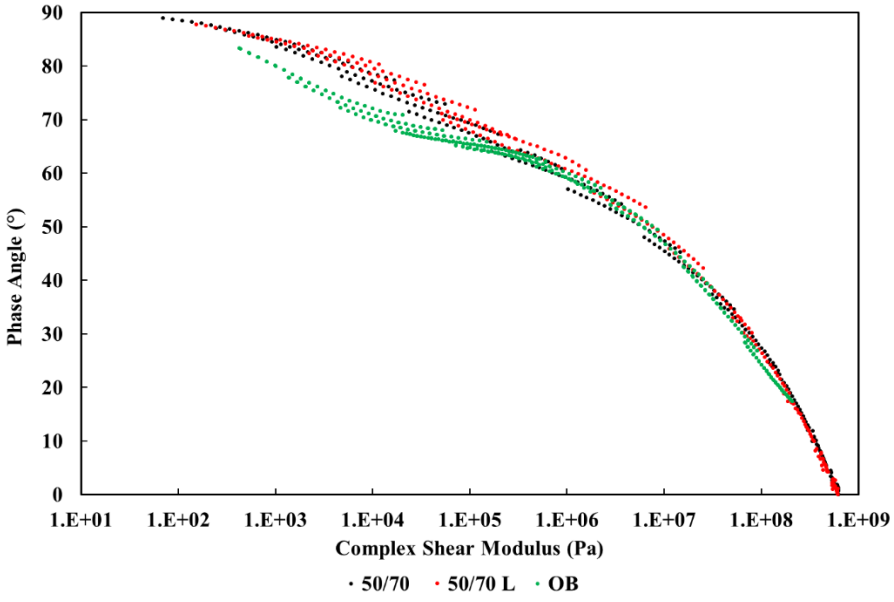

(a) Black diagram of the unaged bitumen

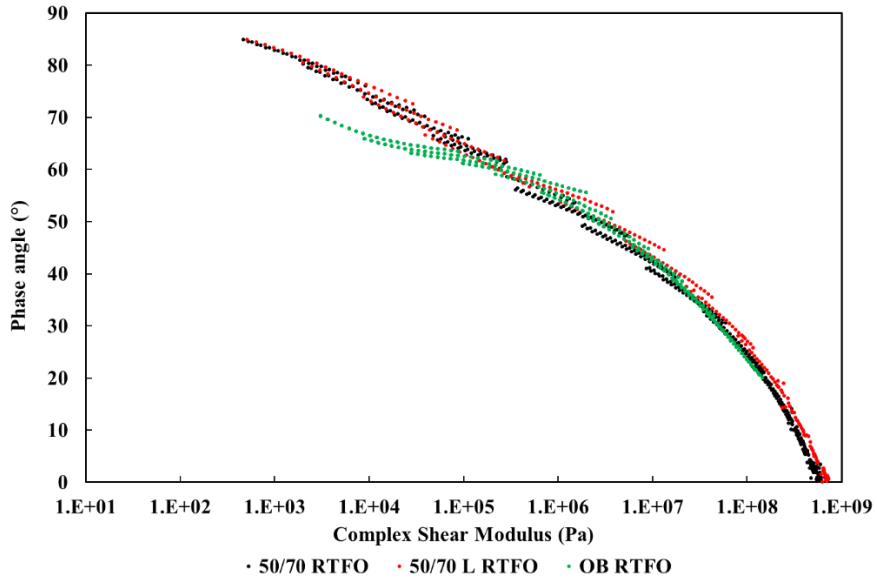

(b) Black diagram of the aged bitumen

Fig. 7 Black diagram of unaged bitumen and aged bitumen

5.2.2 Cole-Cole plots

From Fig. 8, all three unaged binders - 50/70, 50/70 L, and OB - exhibit the characteristic arc-shaped curves typical of bituminous materials, with a distinct peak where the loss modulus (G″) reaches a maximum for a given storage modulus (G′). Overall, the arcs are relatively close to each other, indicating comparable viscoelastic responses in the tested temperature and frequency range. However, minor differences can be observed in the arc positions and peak heights. For instance, the organic bitumen's arc shifts slightly to the right (toward higher G′) compared to 50/70, it suggests that the organic bitumen may be marginally stiffer at equivalent conditions. Conversely, 50/70 L displays a peak in G″ at a lower storage modulus, it could indicate a slightly higher viscous contribution at that point, possibly due to the presence of lignin acting as a filler or mild plasticizer.

For the base 50/70 bitumen, the aged Cole-Cole plot in Fig. 9 reveals a significant reduction in the loss modulus (G″) peak compared to its unaged state. Additionally, the storage modulus (G′) corresponding to the G″ peak shifts slightly to the left and decreases in magnitude, and the overall maximum G′ value also diminishes. This trend indicates that, upon aging, the base bitumen loses part of its energy-dissipating capacity and becomes less stiff, likely due to oxidation-induced degradation of the maltene fraction and the formation of polar oxygenated species that disrupt the original viscoelastic network. In contrast, for both the 50/70 L (lignin-modified bitumen) and the organic bitumen (OB), the aged Cole-Cole plots exhibit an opposite trend. For these binders, the loss modulus (G″) peak significantly increases after aging, and the corresponding storage modulus shifts slightly to the right and increases in value. Notably, the maximum G′ for these binders becomes larger upon aging. In the 50/70 L binder, lignin may act as a reinforcing filler that, despite some plasticizing effects, ultimately promotes additional cross-linking during aging, thus

increasing stiffness and damping. For the organic bitumen, its pure non-petroleum composition means that the bio-based components (such as natural asphalt and bio-oil) undergo oxidation differently from conventional bitumen, possibly forming a more robust network that results in higher G′ and G″ values. These distinct responses highlight how binder composition critically influences aging behavior and long-term performance.

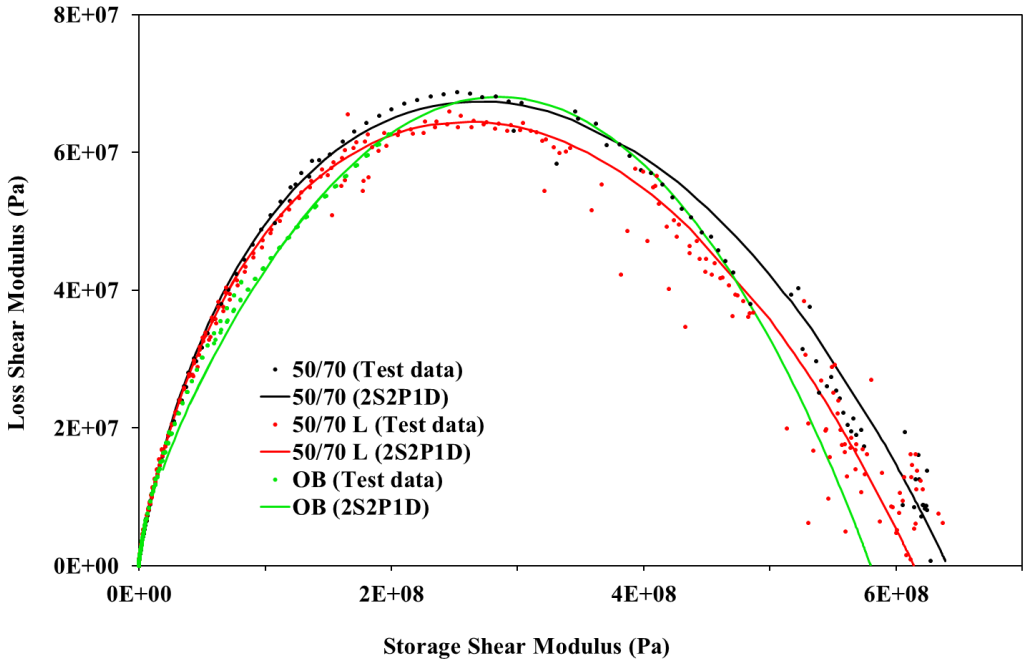

Fig. 8 Cole-Cole plot for the unaged bitumen

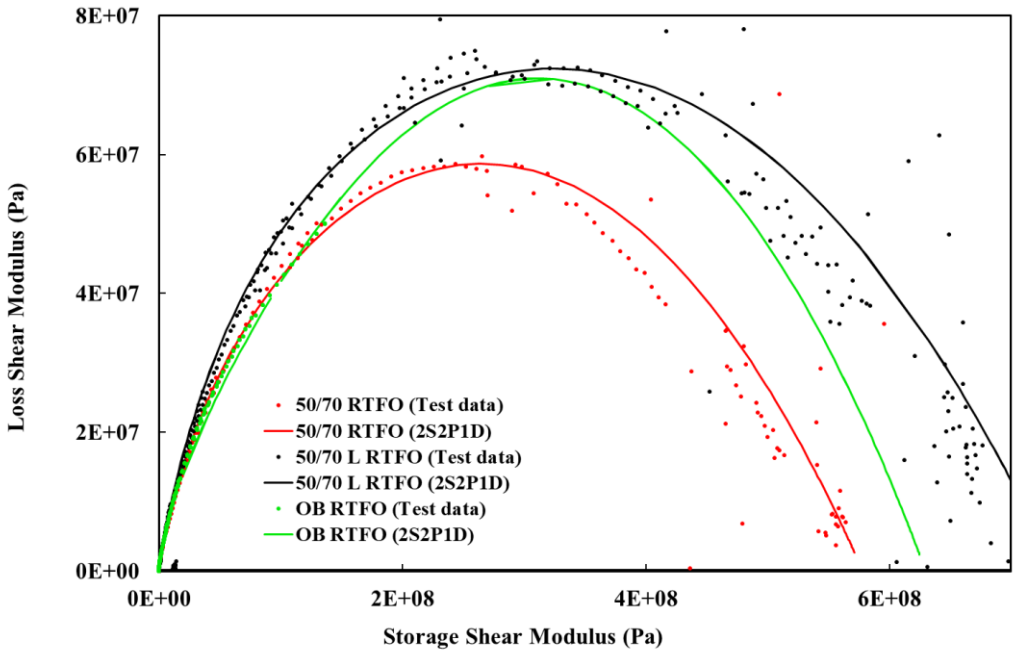

Fig. 9 Cole-Cole plot for the aged bitumen

5.2.3 Master curves of complex modulus and phase angle

Fig. 10 (a) and (b) presents the complex shear modulus G* master curves for the three binders, plotted against the logarithm of reduced frequency at a reference temperature of 20°C. The 2S2P1D model curves closely follow the experimental data points, indicating a strong fit and validating the applicability of this rheological model over a wide range of frequencies. According to the curves, both the lignin-modified bitumen and the organic bitumen exhibit higher G* values than the base 50/70 binder at lower reduced frequencies, which indicates that these two binders are relatively stiffer under slow-loading and/or high-temperature conditions. As the reduced frequency increases (corresponding to lower temperatures or faster loading rates), the three curves tend to converge, suggesting that at higher reduced frequencies the stiffness differences among the binders become less pronounced. In the phase angle plots, the 50/70 binder consistently shows the largest δ across the tested frequency range, implying a more viscous (or less elastic) behavior overall. In contrast, the lignin-modified bitumen and the organic bitumen exhibit lower phase angles, with the organic bitumen generally presenting the lowest δ values among the three binders. This hierarchy—50/70 having the highest phase angles, followed by 50/70 L, and then organic bitumen—indicates that the lignin-modified and bio-based binders are more elastic, whereas the reference bitumen retains a comparatively higher viscous component under the same conditions.

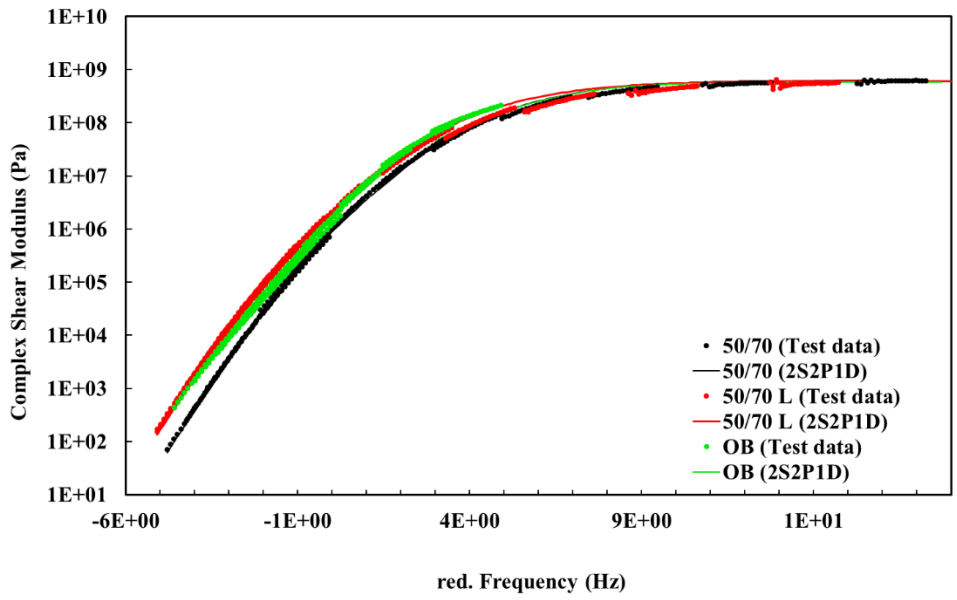

(a) Complex modulus master curves

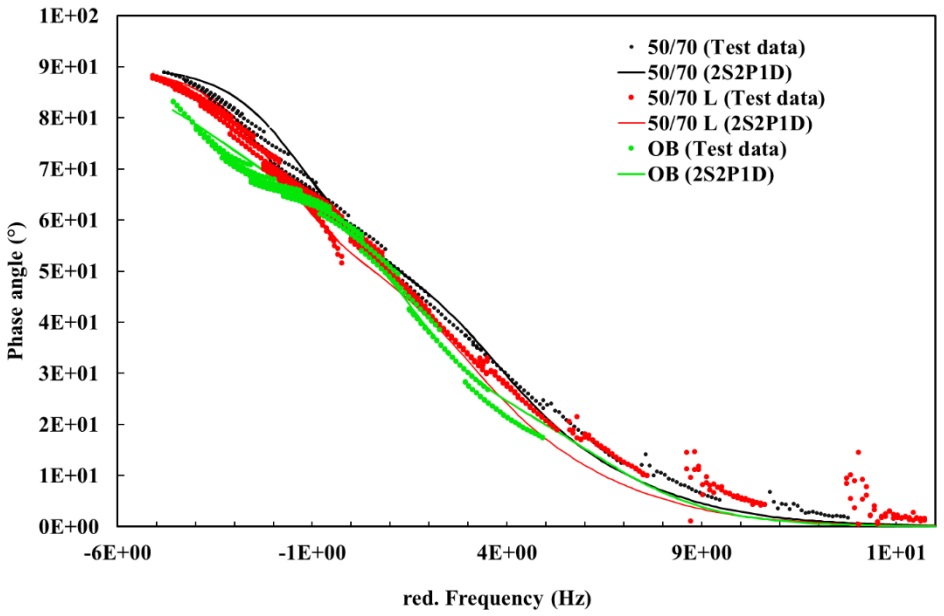

(b) Phase angle master curves

Fig. 10 Master curves of complex modulus and phase angle of three types of unaged bitumen at 20 °C

5.2.4 Aging index analysis

Fig. 11 and Fig. 12 illustrate the complex shear modulus and phase angle of lignin-modified bitumen and organic bitumen in comparison to a base bitumen. In Fig. 11, it can be seen that under unaged conditions, adding lignin enhances the mixture's stiffness across the entire temperature range, functioning similarly to a traditional filler. For instance, at 40 °C, the dynamic shear modulus of unaged lignin-modified bitumen can reach up to 1.8 times that of the base bitumen. However, because lignin has a relatively low specific surface area (1.12 m^2/g), its stiffening effect is comparatively weaker than that of conventional fillers. More notably, this stiffening effect becomes more pronounced after aging, possibly due to certain cross-linking reactions between lignin and bitumen molecules that form a denser three-dimensional network, further increasing the material's stiffness. In contrast, the organic bitumen appears softer than the base bitumen under unaged conditions, likely because the bio-oil component initially acts as a softener. After RTFO aging, however, when the temperature exceeds 20 °C, the organic bitumen's stiffness rises significantly—surpassing even that of the base bitumen (50/70). This phenomenon may stem from disproportionate aging of the bio-oil during RTFO, resulting in partial hardening of the organic bitumen and leading to an additional stiffening effect.

Turning to Fig. 12, which shows the phase angle variations, it is evident that at temperatures above 20 °C, the phase angle indices for all materials remain very close to 1.0, indicating minimal influence from lignin addition or aging on phase angle in that temperature range. In the case of the 50/70 L, the reduction in phase angle observed in the unaged material is similar to that seen after aging. A comparable behavior was also reported by Rochlani et al. (2019) for mastic samples. However, below 40 °C, the organic

bitumen—both aged and unaged—exhibits a higher phase angle, signifying a stronger viscous response at lower temperatures. Taken together, these findings suggest that lignin primarily acts as a filler, improving stiffness by reinforcing intermolecular interactions rather than chemically modifying the bitumen, whereas the bio-oil in the organic bitumen softens the mixture when unaged but experiences significant hardening due to bio-oil oxidation under aging conditions.

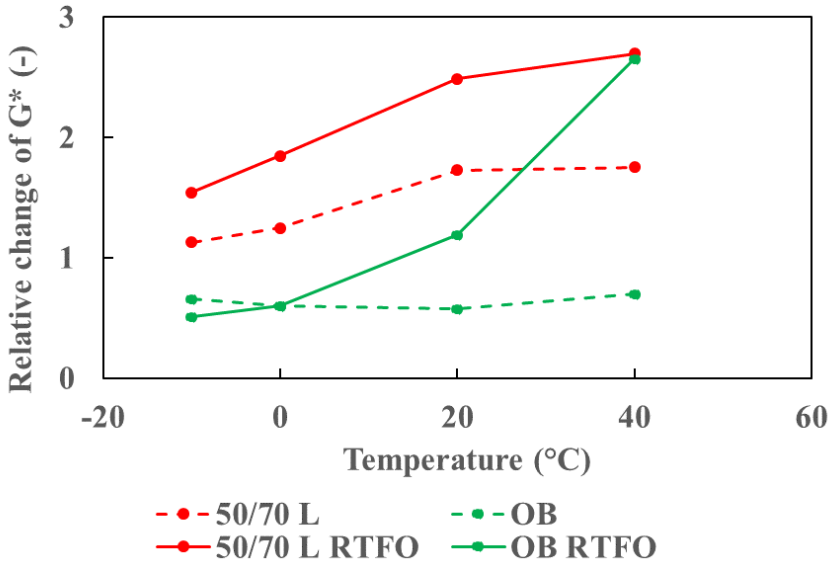

Fig. 11 Changing index of complex shear modulus for the bitumen tested at different temperatures and 10 Hz

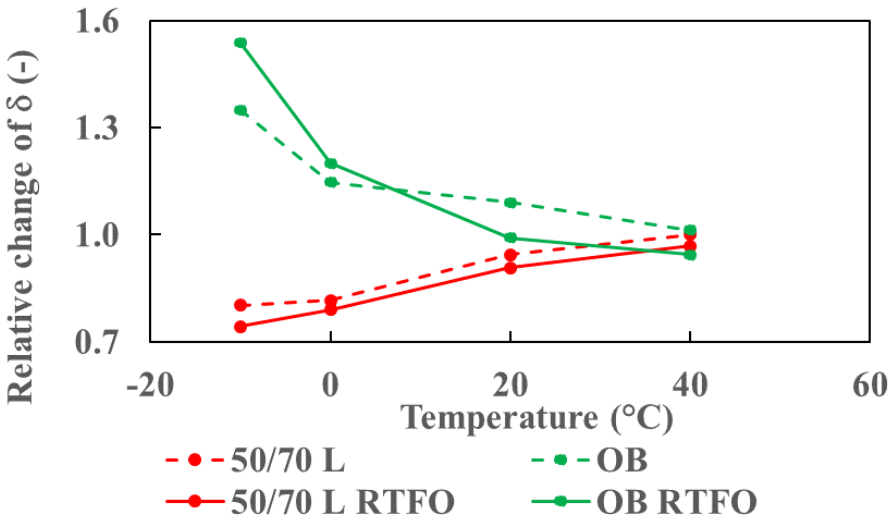

Fig. 12 Changing index phase angle for the bitumen tested at different temperatures and 10 Hz

Furthermore, to quantitatively assess the performance changes of each binder before and after aging, two distinct aging indices were determined. The first index, AI_{G^*}, is based on the complex shear modulus, while the second, AI_{δ}, is derived from the phase angle measurements. Fig. 13 shown the AI_{G^*} of three types of bitumen at four temperatures. The 50/70 L shows stiffening due to RTFO ageing in the investigated temperature range, whereas the other two bitumen become softer at low temperatures (-10°C and 0°C) due to RTFO ageing, i.e. the G* is less than 1. As the temperature rises to 20°C, 50/70 and 50/70 L display

moderate increases in AI_{G^*}, indicating a modest degree of aging-induced stiffening. By contrast, organic bitumen begins to exhibit a more pronounced increase, pointing to greater oxidative or thermal sensitivity in its bio-based components. At 40°C, organic bitumen's AI_{G^*} surpasses 6.0, signifying a markedly higher aging sensitivity at elevated temperatures. This behavior may stem from disproportionate oxidation of the bio-oil fraction or other chemical transformations that occur under high-temperature conditions. In comparison, the AI_{G^*} values for 50/70 and 50/70 L at 40°C are notably lower - around 1.7 and 2, respectively - indicating less pronounced stiffening. Consequently, organic bitumen demonstrates the greatest susceptibility to aging in the high-temperature region, whereas 50/70 L appears more resistant.

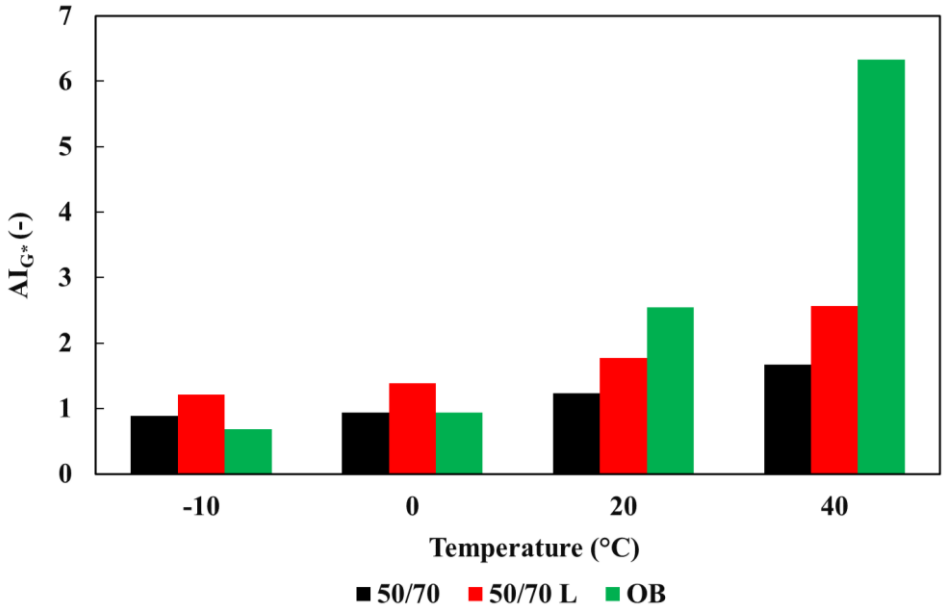

Fig. 13 AI_{G^*} for the bitumen tested

Fig. 14 presents the AI_{δ} for the three binders. For 50/70, the phase angle exhibits only a slight decrease across the entire temperature range, and its AI_{δ} remains close to 1, indicating minimal changes in viscoelastic behavior after RTFO aging. The 50/70 L binder follows a similar trend, and the negligible variance in AI_{δ} between 50/70 and 50/70 L suggests that lignin does not significantly alter the overall phase angle response to aging—both remain near 1 and thus undergo relatively minor reductions in phase angle. In contrast, the organic bitumen displays a pronounced temperature dependence and deviates more noticeably from the other two binders. At certain temperatures, its AI_{δ} differs considerably from 1, implying a more pronounced shift in phase angle following aging. This behavior likely arises from the binder's composition—particularly the asphaltene fraction—which may already be substantially aged or prone to further oxidation under RTFO conditions. As a result, the organic bitumen's phase angle may shift more strongly toward an elastic-dominant response (lower phase angle) or, in some temperature ranges, exhibit a higher viscous component. Overall, all three binders show AI_{δ} below 1.0, consistent with a transition toward a more elastic mode of behavior in the aged state. This shift corresponds to a decrease in phase angle, reflecting the increased stiffness and reduced viscous flow characteristic of oxidative aging.

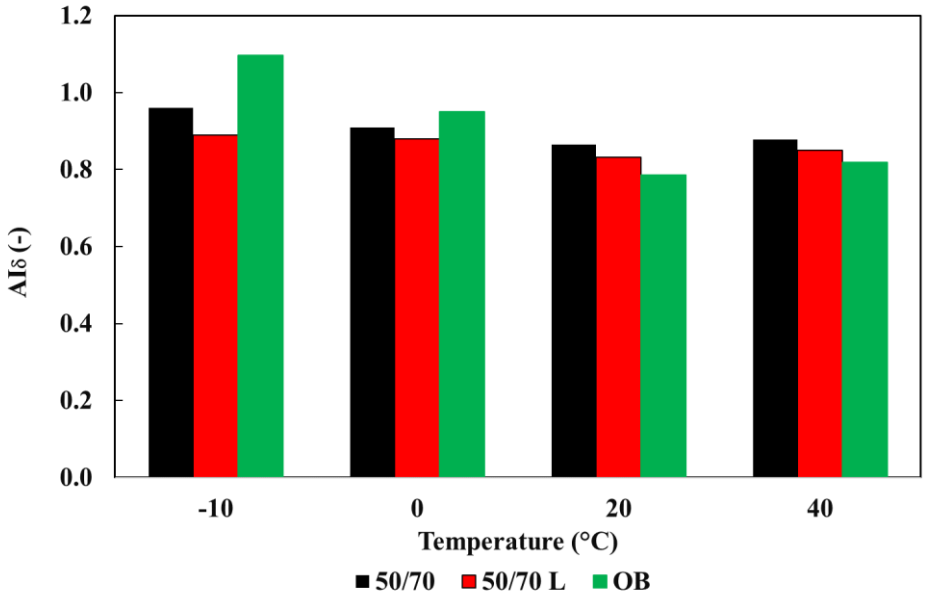

Fig. 14 AI_δ for the bitumen tested

5.3 SSCR tests

Fig. 15 presents the SSCR results—specifically the percentage recovery *R* (left axis) and the non-recoverable creep compliance J_{nr} (right axis)—for the three RTFO-aged binders tested over a temperature range from 40 °C to 80 °C. These parameters provide valuable insight into each binder's ability to resist permanent deformation under repeated loading. In general, a lower J_{nr} value indicates better rutting resistance, while a higher recovery *R* reflects improved elastic behavior. At lower temperatures (e.g., 40 °C), all binders exhibit relatively high *R* values, indicative of strong elastic recovery. However, as the temperature increases toward 80 °C, the binders soften, resulting in decreased recovery and increased non-recoverable compliance. This behavior is consistent with the viscoelastic nature of bituminous materials, which become more fluid-like at elevated temperatures.

Despite this overall trend, notable differences emerge among the three binders. The lignin-modified binder (50/70 L) consistently retains higher *R* values across the tested temperature range compared to conventional 50/70 bitumen. Interestingly, when plotting recovery versus temperature, the curve for the lignin-modified binder exhibits a generally concave shape—similar to that of the 50/70 base bitumen—but shifted upward. In practical terms, this upward shift indicates that, at any given temperature, the lignin-modified binder exhibits higher recovery. However, because the overall shape remains concave rather than becoming convex, it suggests that lignin is not functioning as an active bio-polymer that significantly alters the binder's viscoelastic properties; rather, it appears to act primarily as a filler that slightly enhances recovery without dramatically changing the overall behavior. Furthermore, the organic bitumen (OB) shows an intermediate response: although its recovery decreases at high temperatures, it still outperforms the base

50/70 bitumen in most cases. Meanwhile, the 50/70 binder exhibits the most pronounced drop in *R* and a corresponding increase in J_{nr} with rising temperature, indicating a lower resistance to rutting.

It is also noteworthy that both the organic bitumen and the lignin-modified binder meet the rutting requirements for heavy traffic at temperatures up to 70 °C, as specified by AASHTO M 332-23 (2023) (i.e., Jnr<0.5 kPa−1J), while the base 50/70 binder only fulfills this requirement up to 62 °C. These findings suggest that the incorporation of lignin, even as a filler, and the use of a 100% non-petroleum organic bitumen can both enhance the high-temperature performance and rutting resistance of conventional bitumen.

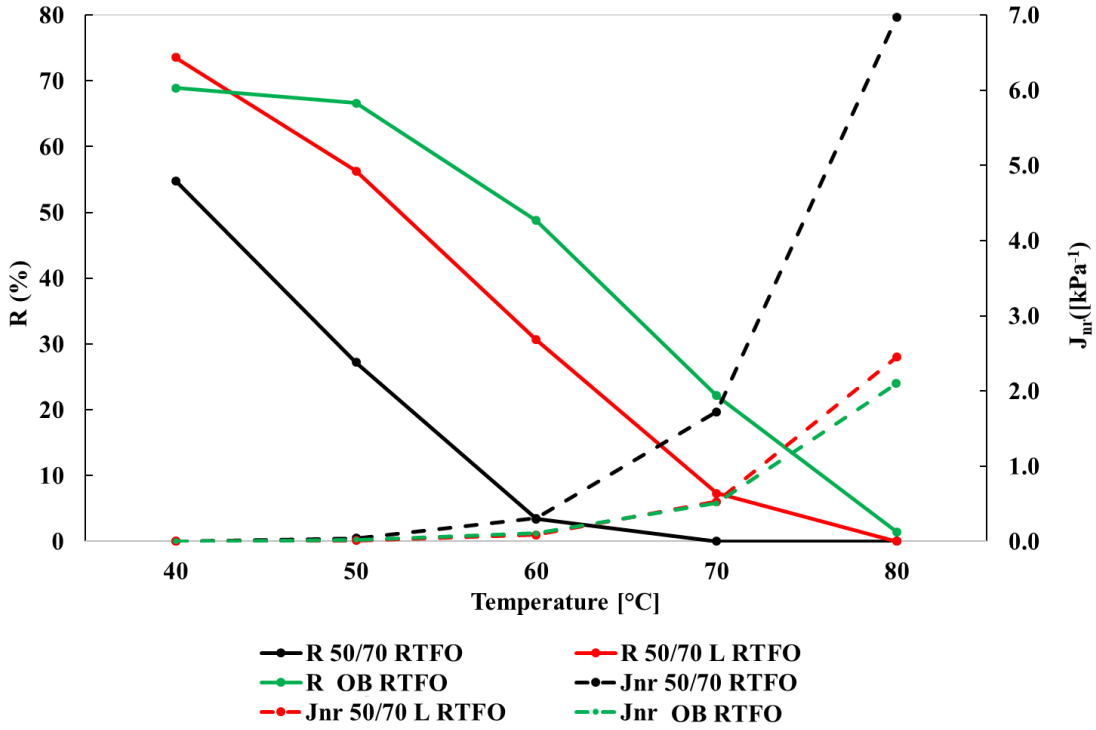

Fig. 15 Results of the SSCR tests

5.4 Life cycle impact assessment

5.4.1 Environmental impact comparison

Since climate change is the only impact category available for organic bitumen, its comparison with bitumen 50/70 and lignin-modified bitumen is limited to this impact category. For all other impact categories, the comparison is conducted solely between the conventional bitumen (50/70) and the lignin-modified bitumen. Additionally, environmental hotspots and trade-offs are identified to provide a comprehensive assessment.

The results for the climate change impact category of conventional bitumen, lignin-modified bitumen and organic bitumen are presented in Fig. 16. The findings indicate that organic bitumen exhibits a nearly 50% lower impact on climate change compared to bitumen 50/70, while lignin-modified bitumen shows a 9.4% reduction. These reductions can be attributed to the reduced crude oil content or its absence, as crude oil is the primary contributor to climate change in conventional and lignin-modified bitumen. However, the

referenced environmental data highlights that the main environmental hotspot for organic bitumen is the transportation of raw materials, which accounts for approximately 97% of the impacts associated with the natural asphalt. Thus, although organic bitumen has a significantly lower climate change impact compared to the other alternatives, optimizing transport distances for raw materials could further enhance its environmental performance.

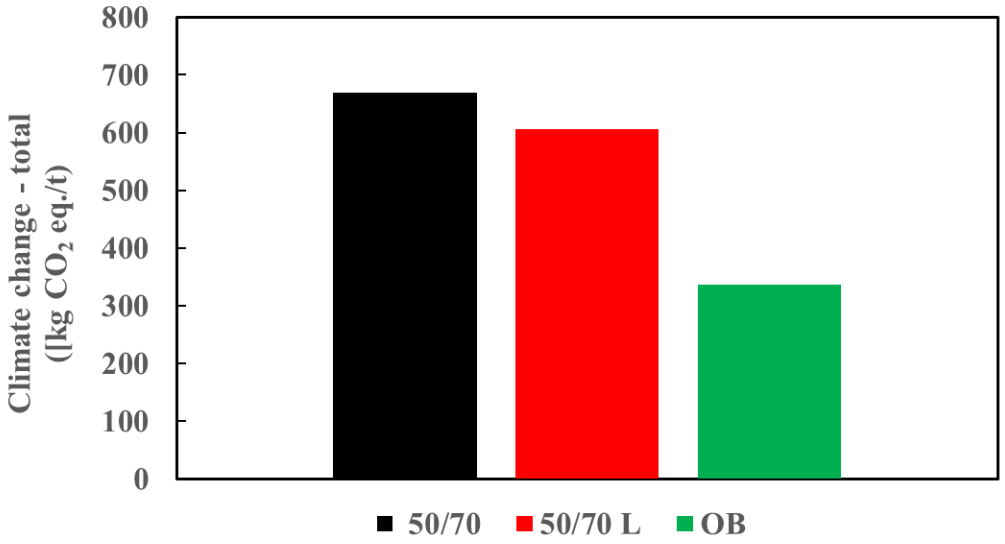

Fig. 16 Climate Change results per declared unit

As detailed in section 4.3, only manufacturer-supplied data was available to characterize climate change for organic bitumen. Therefore, Table 4 presents the LCA results of bitumen 50/70 and lignin-modified bitumen across all impact categories, except for climate change (total), which is reported separately. It can be observed that there is a notable reduction in environmental impacts for lignin-modified bitumen, particularly in the categories of ecotoxicity, eutrophication (freshwater), human toxicity, and resource use (fossils). These reductions are primarily associated with the partial substitution of bitumen with lignin, which lowers the environmental burden from fossil resource extraction. In contrast, conventional bitumen production is strongly linked to the formation of polycyclic aromatic hydrocarbons, which significantly contribute to ecotoxicity and human toxicity, as well as the release of phosphorous and nitrogen compounds, which drive eutrophication impacts. However, lignin-modified bitumen exhibits higher impacts in the categories of climate change (land use and land use change), land use, ozone depletion, ionizing radiation, and water use. These increases are associated with the biomass feedstock requirements for lignin production. Potential mitigation strategies to reduce the land use impact include sourcing biomass from non-forested land. Additionally, selecting feedstocks with lower water demands could help mitigate the water use impact.

Table 4 LCA results per functional unit

Impact category	Unit	50/70	50/70 L
Acidification	[Mole of H+ eq./t]	6.54E+00	5.45E+00
Climate Change, biogenic	[kg CO_2 eq./t]	5.44E+00	4.89E+00
Climate Change, fossil	[kg CO_2 eq./t]	6.63E+02	6.02E+02
Climate Change, land use and land use change	[kg CO_2 eq./t]	7.02E-02	3.05E-01
Ecotoxicity, freshwater - total	[CTUe/t]	2.50E+05	2.01E+05
Eutrophication, freshwater	[kg P eq./t]	7.03E-02	5.67E-02
Eutrophication, marine	[kg N eq./t]	1.62E+00	1.35E+00
Eutrophication, terrestrial	[Mole of N eq./t]	1.75E+01	1.45E+01
Human toxicity, cancer - total	[CTUh/t]	7.28E-07	6.06E-07
Human toxicity, non-cancer - total	[CTUh/t]	3.18E-05	2.66E-05
Ionizing radiation, human health	[kBq U235 eq./t]	3.00E+00	5.56E+00
Land use	[Pt/t]	1.62E+02	3.94E+02
Ozone depletion	[kg CFC-11 eq./t]	3.10E-10	8.86E-10
Particulate matter	[Disease incidences/t]	8.61E-05	7.12E-05
Photochemical ozone formation, human health	[kg NMVOC eq./t]	5.36E+00	4.51E+00
Resource use, fossils	[MJ/t]	4.99E+04	4.16E+04
Resource use, mineral and metals	[kg Sb eq./t]	1.92E-04	1.70E-04
Water use	[m^3 world equiv./t]	5.13E+01	8.05E+01

5.4.2 Interpretation

A sensitivity analysis was performed to evaluate the influence of allocation assumptions regarding the environmental impacts of black liquor. As noted in Chapter 4.1, no direct information on the economic value of black liquor was available and for the baseline scenario an economic value of zero was assumed for this material. For the sensitivity analysis, the economic value of kraft pulp was used as a proxy. Two market values were considered: 10.25 USD/ton, reflecting the market value in January 2025, and 238.40 USD/ton, representing the average market value in 2024 (Procurement Tactics, 2024). For comparison, the market value of kraft paper was assumed to be 572.00 USD/ton (Indexbox, 2024). Based on these values, two allocation factors were derived to assess the environmental impacts of black liquor: 0.17, based on the current Kraft pulp price (first scenario), and 0.29, based on the average Kraft pulp price in 2024 (second scenario). The allocation factors signify that in the first scenario 17% of the environmental impacts from paper production are assigned to black liquor, while in the second scenario 29% of the impacts are assigned to this material. The environmental impacts of black liquor were modeled using the LCI dataset provided by Liang et al. (2023).

The relative change in the environmental impacts of lignin-modified bitumen compared to the baseline scenario (AF = 0) is presented in Table 5. The results indicate that under the considered lignin production

modeling assumptions, the environmental impacts of lignin-modified bitumen increase significantly. The most critical increases occur in the categories of climate change (land use and land use change), land use, ozone depletion, resource use (minerals and metals), and water use. Additionally, when compared to conventional bitumen, lignin-modified bitumen exhibits increased impacts in several categories, including climate change, land use, resource use (fossils and minerals/metals), and water use. These findings highlight the sensitivity of LCA results to assumptions related to lignin production modeling, particularly the need for careful consideration of allocation choice of black liquor.

Table 5 Sensitivity analysis results

Impact category	**Relative change**	
	AF = 0.17	**AF = 0.29**
Acidification	16.51%	28.26%
Climate Change - total	14.03%	24.09%
Climate Change, biogenic	44.26%	75.61%
Climate Change, fossil	12.65%	21.46%
Climate Change, land use and land use change	2388.52%	4063.93%
Ecotoxicity, freshwater - total	1.49%	2.49%
Eutrophication, freshwater	15.14%	25.88%
Eutrophication, marine	21.48%	37.04%
Eutrophication, terrestrial	13.70%	23.29%
Human toxicity, cancer - total	10.73%	18.32%
Human toxicity, non-cancer - total	10.53%	18.05%
Ionizing radiation, human health	28.75%	49.19%
Land Use	1713.78%	2910.20%
Ozone depletion	298763.64%	510127.27%
Particulate matter	18.23%	31.00%
Photochemical ozone formation, human health	11.31%	19.07%
Resource use, fossils	2.17%	3.86%
Resource use, mineral and metals	263.53%	450.00%
Water use	87.58%	149.69%

6. Conclusions and outlook

This study investigated the chemical, rheological of lignin-modified bitumen and organic bitumen including the assessment of their environmental performance as alternatives to conventional petroleum-based bitumen. The key conclusions are as follows:

(1) Fourier-transform infrared spectroscopy (FTIR) analysis revealed that lignin-modified bitumen introduces hydroxyl and aromatic functional groups, influencing its oxidation and aging behavior. In contrast, organic bitumen exhibited distinct spectral features in the fingerprint region, suggesting

organic bitumen follows a distinct oxidation mechanism during aging, potentially forming chemical structures that influence its rheological and durability characteristics. Meanwhile, aging resistance analysis indicated that lignin-modified bitumen demonstrated the least increase in AI_{FTIR} after RTFO aging, suggesting better short-term aging resistance, whereas conventional bitumen exhibited the highest aging susceptibility.

(2) Both lignin-modified and organic bitumen demonstrated higher stiffness and increased elasticity compared to conventional bitumen, as confirmed by Black diagrams, Cole-Cole plots, and master curves. The SSCR test results further indicated superior rutting resistance, with their Jnr values meeting heavy traffic requirements up to 70°C, while conventional 50/70 bitumen was only suitable up to 62°C. However, lignin-modified bitumen exhibited behavior similar to a filler, primarily enhancing stiffness but not significantly altering the overall viscoelastic response. This effect was evident in the Cole-Cole plots, where lignin acted as a reinforcing agent rather than chemically modifying the bitumen structure. In contrast, organic bitumen showed a more elastic response, suggesting stronger molecular interactions that influence its rheological behavior across a wider temperature range.

(3) LCA revealed that organic bitumen provided a nearly 50% reduction in climate change impact, while lignin-modified bitumen achieved a 9.4% reduction, primarily due to their reduced crude oil dependency. However, increased environmental impacts were observed in land use, ozone depletion, and resource consumption, largely attributed to biomass-based raw material sourcing. Sensitivity analysis highlighted that the environmental impact of lignin-modified bitumen is highly dependent on lignin production assumptions, emphasizing the need for optimized biomass sourcing strategies to minimize trade-offs.

Overall, this study underscores the potential of bio-bitumen as a sustainable alternative in road construction, offering enhanced rutting resistance and reduced carbon footprint compared to conventional petroleum-based bitumen. The distinct chemical structure of organic bitumen, particularly its unique spectral features in the fingerprint region, suggests that it undergoes different oxidation and aging mechanisms, which could influence its long-term performance. Further research should focus on the long-term durability, fatigue resistance, and low-temperature behavior of these bio-based binders to ensure their practical implementation in sustainable infrastructure development.

Acknowledgement

The authors gratefully acknowledge the financial support of the German Research Foundation (DFG) SFB/TRR 339, project ID 45359608 and LI 3613/3-1, project ID 528307766. The authors thank the Pontifical Catholic University of Chile for providing the Kraft lignin used in this study and the chemical analysis of the Kraft lignin and Dr. Köberle from TU Dresden for the microscopic images. We also thank the technical staff of the laboratory for their support in preparing and analyzing the samples.

References

AASHTO M 332-23, 2023. Standard Specification for Performance-Graded Asphalt Binder Using Multiple Stress Creep Recovery (MSCR) Test.

Achi, S.S. & Myina, O.M., 2011. Preliminary investigation of Kaduna-Grown cashew nutshell liquid as a natural precursor for dyestuffs, pigments and binders for leather finishing. Nigerian Journal of Chemical Research, 16, 9-14.

Ameli, A. et al., 2021. Investigation of the performance properties of asphalt binders and mixtures modified by Crumb Rubber and Gilsonite. Construction and Building Materials. 279, 122424.

American Association of State Highway and Transportation Officials (AASHTO), 2019. AASHTO T 350 – Standard Method of Test for Multiple Stress Creep Recovery (MSCR) Test of Asphalt Binder Using a Dynamic Shear Rheometer (DSR). Washington, D.C.: AASHTO.

Batista, K.B. et al., 2018. High-temperature, low-temperature and weathering aging performance of lignin modified asphalt binders. Industrial Grops & Products. 111, 107-116.

Boeriu, C.G. et al., 2004. Characterisation of structure-dependent functional properties of lignin with infrared spectroscopy. Industrial Grops & Products. 20, 205-218.

Bruijnincx, P. et al., 2016. Lignin valorisation: The importance of a full value chain approach. Utrecht, Netherlands: Utrecht Univ.

Del Rosario, P., & Traverso, M., 2023. Towards sustainable roads: a systematic review of triple-bottom-line-based assessment methods. Sustainability, 15, 15654.

Elahi, Z. et al., 2024. Influence of novel modified waste cooking oil beads on rheological characteristics of bitumen. Construction and Building Materials. 414, 134829.

Eurobitume. The Eurobitume Life-Cycle Inventory for Bitumen. Version 3.1. Brussels, Belgium: European Bitumen Association. 2020.

European Committee for Standardization, 2014. EN 12607-1: Bitumen and bituminous binders – Determination of the resistance to hardening under the influence of heat and air – Part 1: RTFOT method. Brussels: CEN.

Fachagentur Nachwachsende Rohstoffe. (2024). Basisdaten Wald und Holz 2025. Fachagentur Nachwachsende Rohstoffe e.V. (FNR). https://www.fnr.de/fileadmin/Projekte/2025/Mediathek/Brosch_Basisdaten_W_H_2025_web.pdf

Gaudenzi, E. et al., 2023. The use of lignin for sustainable asphalt pavements: A literature review. Construction and Building Materials. 362, 129773.

Global Bioeconomy Summit 2020. (2020). Global Bioeconomy Policy Report (IV): a decade of bioeconomy policy development around the world.

Ibrahim, M.N.M. et al., 2019. Synthesis of lignin based composites of TiO2 for potential application as radical scavengers in sunscreen formulation. BMC Chemistry. 13, 17

Indexbox, 2024. Uncoated Kraft Liner Market in the United States. https://app.indexbox.io/report/480411h480419/840/?_gl=1*tb6bii*_ga*NDM3NTc5MTAyLjE3Mzc2NTI3Mjg.*_ga_6KCVGEDSJE*MTczNzcwOTE2Ny4yLjEuMTczNzcwOTE3Ny4wLjAuMA..

ISO, 2006a. Environmental management — Life cycle assessment — Principles and framework. (ISO 14040:2006).

ISO, 2006b. Environmental management — Life cycle assessment — Requirements and guidelines (ISO 14044:2006).

Kyei, S. K. et al., 2019. Extraction, characterization and application of cashew nut shell liquid from cashew nut shells", Chemical Science International Journal. 28, 1–10.

Li, R. et al., 2022. Microstructure characterisation and constitutive modelling of waterborne epoxy resin modified bitumen emulsion. International Journal of Pavement Engineering. 23, 5077-5086.

Liang, J. et al., 2023. Performance comparison of black liquor gasification and oxidation in supercritical water from thermodynamic, environmental, and techno-economic perspectives. Fuel. 334, 126787.

Liljenström, C. et al., 2022. Including maintenance in life cycle assessment of road and rail infrastructure—a literature review. The International Journal of Life Cycle Assessment, 27, 316–341.

Lin, H.T. et al., 2022. Characterization of rheological properties and aging performance of bitumen modified by bio-oil from bamboo charcoal production. Journal of Cleaner Production. 338, 130678.

Mirwald, J. et al., 2022. Comparison of microscopic techniques to study the diversity of the bitumen microstructure. Micron. 159, 103294.

Mantau, U., 2013. Umsatzentwicklung energetischer Holzverwendung in Deutschland 2000 bis 2012 – Abschlussbericht. https://literatur.thuenen.de/digbib_extern/dn053145.pdf

Nahar, S. et al., 2022. Mutual compatibility aspects and rheological assessment of (modified) lignin–bitumen blends as potential binders for asphalt. Road Materials and Pavement Design. 24, 2379–2392.

Ncir, N. et al., 2014. Chemical characterization of gilsonite bitumen. Journal of Petroleum & Environmental Biotechnology. 5, 1-10.

Pahlavan, F. et al., 2024. From biowaste to BioPave: Biological pathways for sequestration of anthropogenic CO_2 and enhancing durability of roadway infrastructures. Resources, Conservation & Recycling. 205, 107515.

Pakdaman, E. et al., 2019. Production of hydrophilic gilsonite nanoparticles using surface modification and planetary ball mill processes. The 16th Iranian National Congress of Chemical Engineering.

Parvan, M., 2023. Life cycle assessment of lignin recovery in a kraft pulp mill and its alternative ways of utilization. Master Thesis, LUT University.

Pascoal, A. et al., 2023. Improvement of warm-mix asphalt concrete performance with lignin obtained from bioethanol production from forest biomass waste. Materials. 16, 7339.

Procurement Tactics. (2024). Kraft pulp prices – Historical Graph. https://procurementtactics.com/kraft-pulp-prices/

Ribeiro, E.L. et al., 2012. Evaluation of moisture damage in asphalt containing cashew nut shell liquid (CNSL) modified bitumen. A5EE-386, 5th Eurasphalt & Eurobitume Congress, Istanbul. 2012.

Rochlani, M. et al., 2019. Influence of filler properties on the rheological, cryogenic, fatigue and rutting performance of mastics. Journal of Construction and Building Materials. Volume 227.

Rondón-Quintana, H.A. et al., 2023. Natural Asphalts in Pavements: Review. Sustainability. 15, 2098.

Somé, S.C. et al., 2016. Evaluation of the potential use of waste sunflower and rapeseed oils-modified natural bitumen as binders for asphalt pavement design. International Journal of Pavement Research and Technology. 9, 368-375.

Sabouri, M. et al., 2018. Effectiveness of Linear Amplitude Sweep (LAS) asphalt binder test in predicting asphalt mixtures fatigue performance. Construction and Building Materials. 171, 281-290.

Singh, A. Gupta, A. & Milijkovic, M. 2023. Intermediate- and high temperature damage of bitumen modified with HDPE from various sources. Road Materials and Pavement Design 24: 640-653.

Srivastava R. & Srivastava D., 2015Mechanical, chemical, and curing characteristics of cardanol–furfural-based novolac resin for application in green coatings. Journal of Coatings Technology and Research, 12, 303-311.

Sun, H.D. et al., 2022. Study on performance optimization of composite natural asphalt modified gussasphalt mix. Coatings. 12, 78.

Sun, Z. et al., 2016. Properties of asphalt binder modified by bio-oil derived from waste cooking oil. Construction and Building Materials. 102, 496-504.

Terrel, R. Evaluation of wood lignin as a substitute or extender of asphalt, U.S. Department of Transportation - Federal Highway Administration, Washington DC, 1980.

Tokede, O.O. et al., 2020. Life cycle assessment of asphalt variants in infrastructures: The case of lignin in Australian road pavements. Structures. 25, 190-199.

Wang, H.N. et al., 2020. Preparation process of bio-oil and bio-asphalt, their performance, and the application of bio-asphalt: A comprehensive review. Journal of Traffic and Transportation Engineering (English Edition). 7, 137-151.

Xu, N. et al., 2023. Research progress on resource utilization of waste cooking oil in asphalt materials: A state-of-the-art review. Journal of Cleaner Production. 385, 135427.

Zhang, R. et al., 2020. Modification mechanism of using waste wood–based bio-oil to modify petroleum asphalt. Journal of Materials in Civil Engineering. 32, 04020375.

Zhang, Y. et al., 2025. Life cycle assessment of bio-bitumen production: A case study in China. Journal of Traffic and Transportation Engineering (English Edition), 12, 123-134.